

# Untangling featural and conceptual object representations

Tijl Grootswagers<sup>1,2,^</sup>, Amanda K. Robinson<sup>1,2</sup>, Sophia M. Shatek<sup>1</sup>, Thomas A. Carlson<sup>1</sup>

<sup>1</sup> School of Psychology, University of Sydney, Sydney, NSW, Australia

<sup>2</sup> Perception in Action Research Centre, Macquarie University, Sydney, NSW, Australia

<sup>^</sup> Corresponding author: [tijl.grootswagers@sydney.edu.au](mailto:tijl.grootswagers@sydney.edu.au)

## Abstract

How are visual inputs transformed into conceptual representations by the human visual system? The contents of human perception, such as objects presented on a visual display, can reliably be decoded from voxel activation patterns in fMRI, and in evoked sensor activations in MEG and EEG. A prevailing question is the extent to which brain activation associated with object categories is due to statistical regularities of visual features within object categories. Here, we assessed the contribution of mid-level features to conceptual category decoding using EEG and a novel fast periodic decoding paradigm. Our study used a stimulus set consisting of intact objects from the animate (e.g., fish) and inanimate categories (e.g., chair) and scrambled versions of the same objects that were unrecognizable and preserved their visual features (Long, Yu, & Konkle, 2018). By presenting the images at different periodic rates, we biased processing to different levels of the visual hierarchy. We found that scrambled objects and their intact counterparts elicited similar patterns of activation, which could be used to decode the conceptual category (animate or inanimate), even for the unrecognizable scrambled objects. Animacy decoding for the scrambled objects, however, was only possible at the slowest periodic presentation rate. Animacy decoding for intact objects was faster, more robust, and could be achieved at faster presentation rates. Our results confirm that the mid-level visual features preserved in the scrambled objects contribute to animacy decoding, but also demonstrate that the dynamics vary markedly for intact versus scrambled objects. Our findings suggest a complex interplay between visual feature coding and categorical representations that is mediated by the visual system's capacity to use image features to resolve a recognisable object.

## 25 Introduction

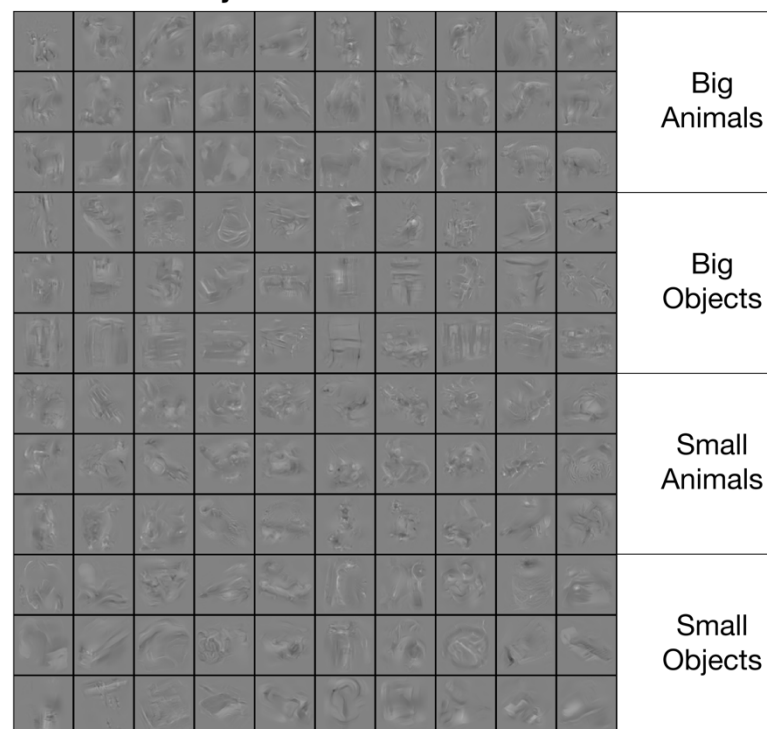
26 How does the brain transform perceptual information into meaningful concepts and categories? One key  
 27 organisational principle of object representations in the human ventral temporal cortex is animacy (Caramazza &  
 28 Mahon, 2003; Caramazza & Shelton, 1998; Kiani, Esteky, Mirpour, & Tanaka, 2007; Kriegeskorte et al., 2008;  
 29 Mahon & Caramazza, 2011; Spelke, Phillips, & Woodward, 1995). Operationalised as objects that can move on  
 30 their own volition, animate objects evoke different activation patterns than inanimate objects in human brain  
 31 activity patterns in fMRI (Cichy, Pantazis, & Oliva, 2014; Connolly et al., 2012; Downing, Jiang, Shuman, &  
 32 Kanwisher, 2001; Grootswagers, Cichy, & Carlson, 2018; Konkle & Caramazza, 2013; Kriegeskorte et al., 2008)  
 33 and in MEG/EEG (Carlson, Tovar, Alink, & Kriegeskorte, 2013; Contini, Wardle, & Carlson, 2017;  
 34 Grootswagers, Ritchie, Wardle, Heathcote, & Carlson, 2017; Grootswagers, Robinson, & Carlson, 2019;  
 35 Kaneshiro, Guimaraes, Kim, Norcia, & Suppes, 2015; Ritchie, Tovar, & Carlson, 2015). A current debate concerns  
 36 the degree to which categorical object representations are due to systematic featural differences within categories  
 37 (Long et al., 2018; op de Beeck, Haushofer, & Kanwisher, 2008; Proklova, Kaiser, & Peelen, 2016).

38 Recent work has focused on understanding the contribution of visual features to the brain's representation of  
 39 categories, such as animacy. This work has shown that a substantial proportion of animacy coding can be explained  
 40 by low and mid-level visual features (e.g., texture and curvature) that are inherently associated with animate versus  
 41 inanimate objects (Andrews, Watson, Rice, & Hartley, 2015; Bracci, Kalfas, & Op de Beeck, 2017; Bracci & Op  
 42 de Beeck, 2016; Bracci, Ritchie, & de Beeck, 2017; Coggan, Liu, Baker, & Andrews, 2016; Kaiser, Azzalini, &  
 43 Peelen, 2016; Long et al., 2018; Proklova et al., 2016; Rice, Watson, Hartley, & Andrews, 2014; Ritchie, Bracci, &  
 44 op de Beeck, in press; Watson, Young, & Andrews, 2016). Long et al. (2018) recently investigated how mid-level  
 45 features contribute to categorical representations using images of intact objects and scrambled "texform" versions  
 46 of the same objects. Crucially, the texform versions of the objects were unrecognisable but preserved mid-level  
 47 features such as texture. Using fMRI, they found the categories of animacy and size were similarly coded in the  
 48 brain for intact and texform versions of objects, thus demonstrating that such representations can arise without  
 49 the explicit recognition of an object (Long et al., 2018). In MEG and EEG, one study showed that animate and  
 50 inanimate objects cannot be differentiated when they are closely matched for shape (Proklova, Kaiser, & Peelen,  
 51 2019). Other studies, however, have found that object animacy decoding generalises to unseen exemplars with

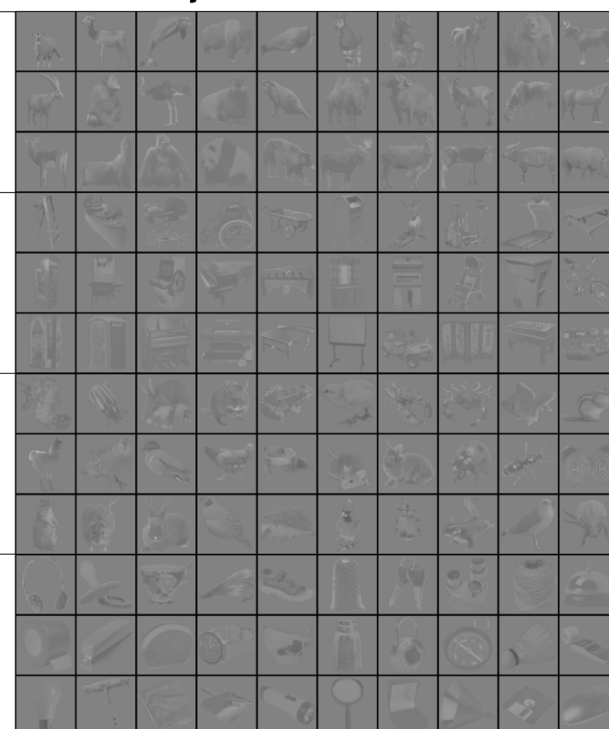
different shapes (cf. Contini et al., 2017), suggesting animacy decoding, in part, might be based on general conceptual representations. Taken together, these results suggest that either there is some abstract conceptual representation of animacy, or that objects within the animate and inanimate categories share sufficient visual regularities to drive the categorical organisation of object representations in the brain.

In the current study, we tested the contribution of visual features to the dynamics of emerging conceptual representations. We used a previously published stimulus set (Figure 1) that was designed to test the contribution of mid-level features to conceptual categories (animacy and size) in the visual system (Long et al., 2018), which consisted of luminance-matched real objects, and scrambled, “texform” versions of the same objects that retain mid-level texture and form information (Long, Störmer, & Alvarez, 2017; Long et al., 2018). To determine the extent to which the conceptual categories of the intact objects are driven by mid-level features preserved in the texforms, we used EEG and a rapid-MVPA paradigm (Grootswagers et al., 2019). Previous work using this paradigm has shown that the presentation rate limited the depth of object processing (Grootswagers et al., 2019; Robinson, Grootswagers, & Carlson, 2019). In this study, we similarly varied presentation rates to study how the emergence of categorical information is affected by the processing time devoted to each image. We found that EEG activation patterns of texform versions of the animate and inanimate objects were decodable, but that animacy decoding of intact objects was more robust, and could be achieved at faster presentation rates. Together, our results provide evidence that visual features contribute to the representation of object categories, but higher level abstraction cannot be achieved from statistical regularities alone.

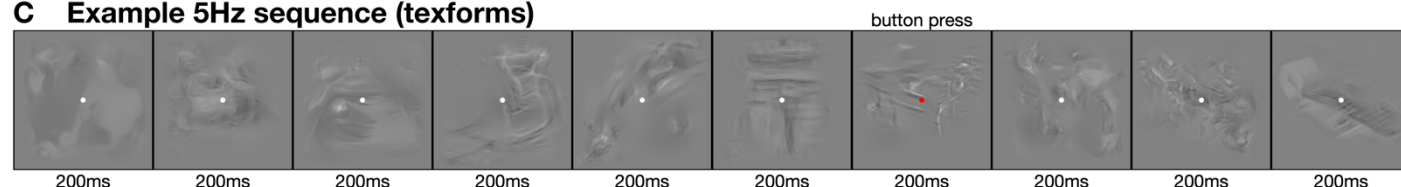
## A Texform objects



## B Intact objects



## C Example 5Hz sequence (texforms)



## D Example 5Hz sequence (intact objects)

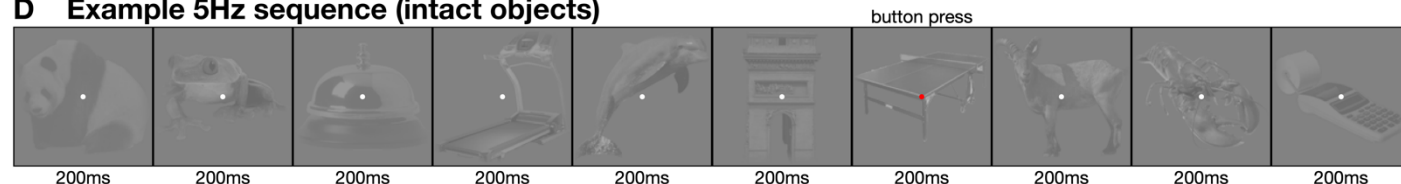
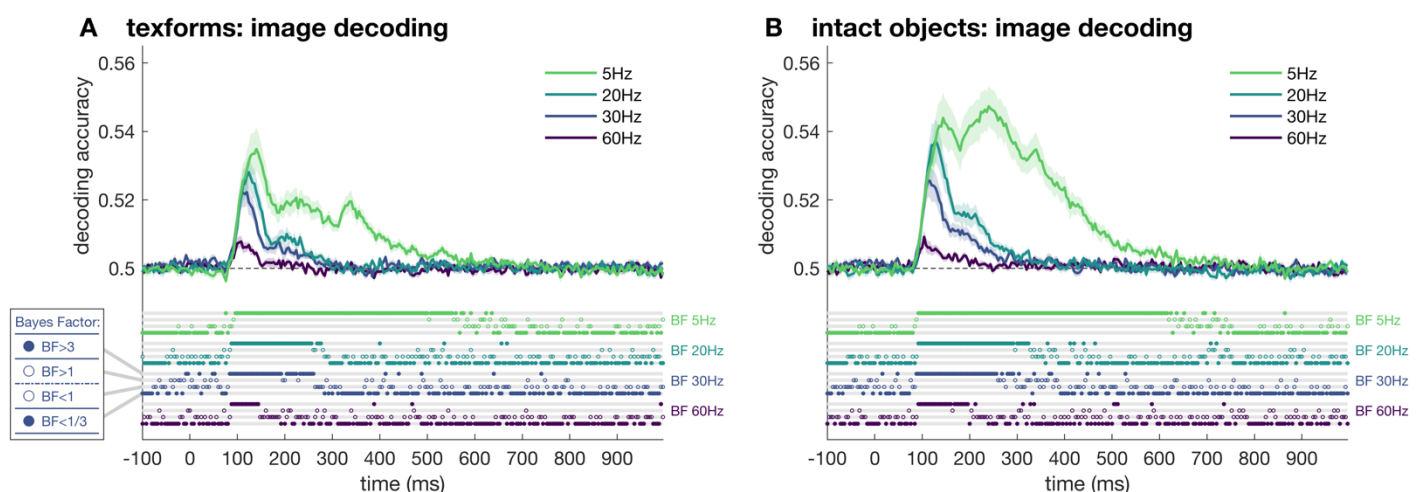


**Figure 1. Stimuli and design.** Stimuli were 120 objects categorizable as animate or inanimate, and as big or small. A. The first half of the experiment used texform versions of objects (presented first so that participants were not aware of their intact counterparts). B. In the second half of the experiment, the original intact versions were used. All images were obtained from <https://osf.io/69pbd/> (Long et al., 2018). Stimuli were presented at four presentation frequencies. C. Example texform sequence at 5Hz, where stimuli were presented for 200ms each. D. Example intact object sequence at 5Hz. The sequence presentation orders for intact objects and texforms were matched. Participants performed an orthogonal task where they responded with a button press to the fixation dot turning red.

## 80 Results

81 Participants (N=20) viewed streams of texform stimuli and intact objects (Figure 1). The stimuli were presented  
 82 in random order at four presentation frequencies (60Hz, 30Hz, 20Hz, 5Hz) to target different levels of visual  
 83 processing (Grootswagers et al., 2019; Robinson et al., 2019). The stimuli were developed by Long et al., (2017),  
 84 and obtained from <https://osf.io/69pbd/> (Long et al., 2017, 2018). Continuous EEG was recorded during the  
 85 streams and cut into overlapping epochs based on the onset of each stimulus within the streams. The epoched  
 86 data were subjected to a multivariate decoding analysis, similar to previous work that decoded individual images  
 87 in fast presentation streams (Grootswagers et al., 2019; Robinson et al., 2019).

88 To investigate how image representations differed between the texform and intact versions, we obtained cross-  
 89 validated classifier performance between all pairwise texform images (Figure 2A), and all pairwise intact object  
 90 images (Figure 2B). Both texforms and intact objects were decodable from around 90 ms after stimulus onset at  
 91 all presentation frequencies, characteristic of early stages of visual processing (Carlson et al., 2013; Cichy et al.,  
 92 2014; Contini et al., 2017). Faster presentation frequencies resulted in lower peak decoding and shorter decoding  
 93 durations, consistent with previous results showing that fast rates restrict visual processing (Robinson et al., 2019).  
 94 In sum, the image-level decoding results were similar between texforms and intact objects, apart from the intact  
 95 objects at 5Hz, where a larger second peak was observed that was not apparent for the texforms.



96 **Figure 2. Decoding texforms and intact objects.** **A.** Decoding between all texform image pairs. **B.** Decoding  
 97 between all intact object image pairs. Different lines in each plot show decoding accuracy for different presentation  
 98 frequencies over time relative to stimulus onset, with shaded areas showing standard error across subjects (N=20).  
 99 Thresholded Bayes factors (BF) for above-chance decoding are displayed above the x-axes for every time point as  
 00 an open or closed circle in one of four locations (see inset).  
 01

To investigate to what extent the visual features preserved in the texform versions of the objects drive categorical distinctions in activation patterns, we trained classifiers on decoding animacy from the stimuli, using an exemplar-by-sequence cross-validation approach to avoid overfitting to individual images (Carlson et al., 2013; Grootswagers et al., 2019). For texforms, above chance decoding of (featural) animacy was observed between 300ms and 400ms after stimulus onset (Figure 3A) for the 5Hz presentation frequency but was not evident for the faster presentation rates. Animacy of the intact object images, in contrast, could be decoded above chance for 5Hz, 20Hz and 30Hz (Figure 3B). Onset of animacy decoding was approximately 150ms for the 5Hz and 20Hz conditions, and at 220ms for the 30Hz frequency. This result shows that the shared visual features between texforms and intact objects contributes to, but do not wholly explain, the categorical representation of animacy in the brain.

In the final analysis, we asked if the categorical representation of real-world size emerges similarly for intact and texform versions of objects. An exemplar-by-sequence cross-validation approach was used to decode real world size (small versus large objects) for the texform and intact objects. At none of the presentation rates was (featural) real-world size decodable from the texform stimuli (Figure 4A). Real world size of the intact object images was decodable for 5Hz and 20Hz frequencies (Figure 4B). Combined, the animacy and size decoding results show a fundamental difference in how conceptual categories emerge for intact objects and their scrambled counterparts.

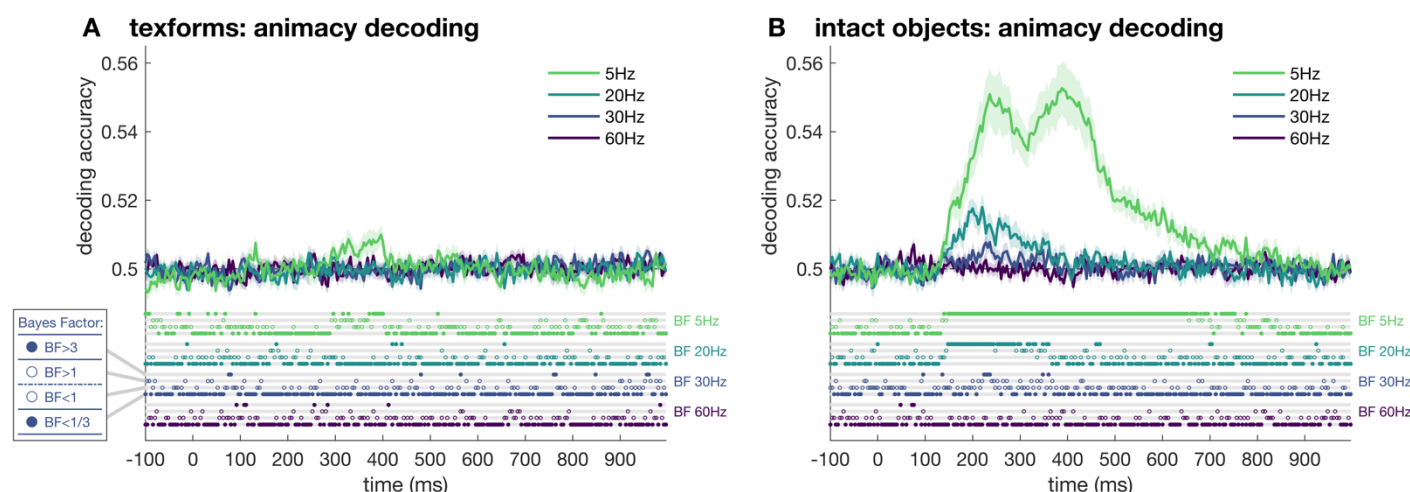


**Figure 3. Animacy was decodable from texforms, but stronger from intact images. A.** Decoding the animacy of the texform images. **B.** Decoding the animacy of the intact objects. Different lines in each plot show decoding accuracy for different presentation frequencies over time relative to stimulus onset, with shaded areas showing standard error across subjects (N=20). Thresholded Bayes factors (BF) for above-chance decoding are displayed above the x-axes for every time point as an open or closed circle in one of four locations (see inset).



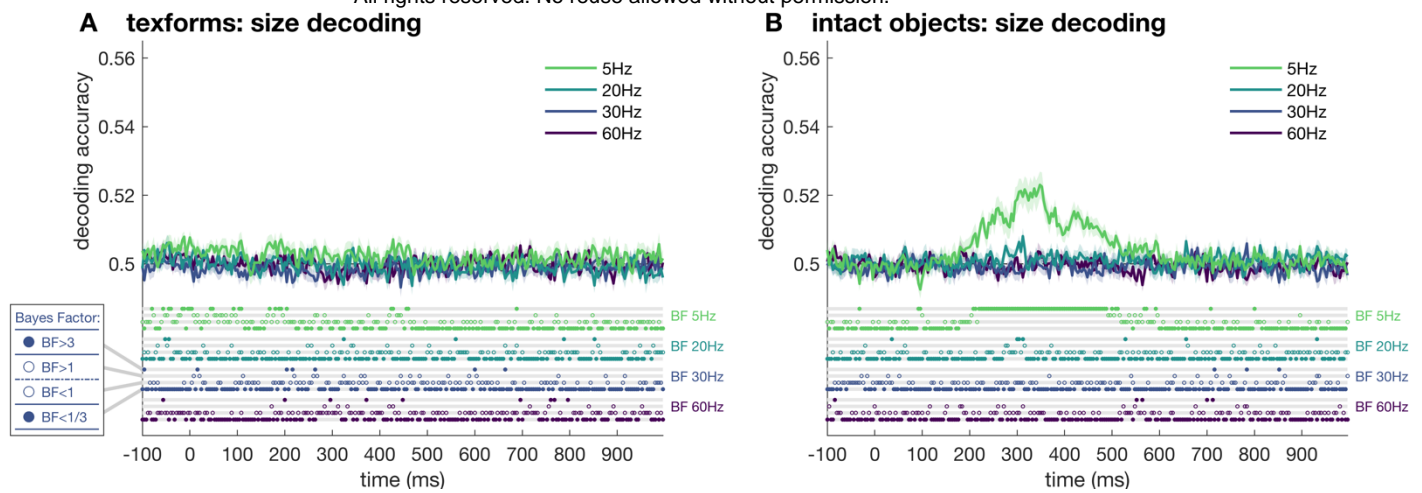


**Figure 4. Size was only decodable from intact objects. A.** Decoding the real-world size of the texform images. **B.** Decoding the real-world size of the intact objects. Different lines in each plot show decoding accuracy for different presentation frequencies over time relative to stimulus onset, with shaded areas showing standard error across subjects ( $N=20$ ). Thresholded Bayes factors (BF) for above-chance decoding are displayed above the x-axes for every time point as an open or closed circle in one of four locations (see inset).

## Discussion

In this study, we assessed the contribution of mid-level features to high level categorical object representations using a combination of fast periodic visual processing streams and multivariate EEG decoding. We used images of intact and texform versions of objects from a previously published study (Long et al., 2018) and found that their neural representations were similarly distinct at the image level. In contrast, the decoding accuracies of the original categorical distinctions of animacy and real-world size varied markedly across the texform and intact versions of the objects. The patterns of neural activity evoked by animate and inanimate intact objects were decodable during a larger time period than their texform versions, suggesting the temporal dynamics of animacy varied despite the maintenance of mid-level visual features. In addition, the animacy of intact objects was decodable at 5Hz, 20Hz and 30Hz, but texforms were only decodable at 5Hz. Higher level categorical brain regions exhibit larger responses to slower presentation rates relative to faster rates (McKeeff, Remus, & Tong, 2007), and we previously found that slower object presentations reached higher, more abstract levels of visual processing (Grootswagers et al., 2019). Thus, the absence of animacy decoding for texform objects at faster presentation rates indicates that higher level processing was required for the animate/inanimate distinction in texform stimuli. We interpret these findings as evidence that shared visual features between texforms and intact objects contribute to, but do not wholly explain, the categorical organisation of animacy in the brain.

Our results corroborate fMRI results using the same stimuli showing that texforms and intact objects generated similar categorical representations along the visual hierarchy but that the recognizable images generated stronger category responses (Long et al., 2018). The current results further show a clear difference in the temporal dynamics of animacy representations within the visual system for featural versus conceptual object representations. At faster presentation rates, animacy decoding was observed in intact objects but not in texforms, indicating that intact objects promote categorical representations with limited processing. It is important to note that the intact objects were shown only in the second half of the experiment, which might have contributed to better animacy decoding for intact objects. However, image-level results were similar between texforms and intact objects, which suggests that the experimental paradigm was not wholly responsible for the differences in categorical-level decoding. Together, these results suggest that brain responses to intact objects contain additional animacy category information over and above the statistical visual regularities present in the texforms.

The texform scrambling process was used to render images unrecognisable, while maintaining featural image statistics. Some low-level visual information may have been lost in the scrambling process, such as shape and curvature information, which is a strong cue for animacy (Levin, Takarae, Miner, & Keil, 2001; Schmidt, Hegele, & Fleming, 2017; Zachariou, Giacco, Ungerleider, & Yue, 2018). In MEG and EEG decoding studies, classification can be strongly driven by differences in object shape (Proklova et al., 2019), and silhouette similarity is often a strong predictor of the similarities between the earliest neural responses (Carlson et al., 2013; Grootswagers et al., 2019; Teichmann, Grootswagers, Carlson, & Rich, 2018; Wardle, Kriegeskorte, Grootswagers, Khaligh-Razavi, & Carlson, 2016). Furthermore, human categorisation accuracies on (synthesised) images was found to be predicted by the amount of curvilinear and rectilinear information in the image (Zachariou et al., 2018). Yet, even if intermediate visual features are sufficient to classify conceptual categories above-chance behaviourally, our results suggest that this is only possible given sufficient processing time.

These findings support the notion that large-scale categorical organisations in the visual system are to some extent driven by mid-level visual features. However, if concepts were decodable using only brain responses to mid-level feature, then this would predict above-chance decoding of concepts also at faster frequencies for the texforms. This was not the case in our results. Instead, we only observed animacy decoding for the slowest (5Hz) presentation frequency, which suggests that the conceptual animacy category only emerges from mid-level features



72 after deeper processing. Thus, it could be the case that mid-level feature coding in early visual areas does not allow  
 73 for concept decoding, but these features are “untangled” by higher visual areas into linearly separable categorical  
 74 organisations (DiCarlo & Cox, 2007). This would mean that visual features could indeed drive the organisation in  
 75 high level areas, but only given sufficient processing time for such these untangling processes to complete.  
 76 Furthermore, the speed of processing or information transfer to these higher visual areas could be modulated by  
 77 the amount of evidence that supports the successful recognition of an object. For example, the intact objects have  
 78 a well-defined outline that separates the object from the background, while the edges of the texforms are more  
 79 blurred. This potentially could disrupt segmentation processes which in turn delays the amount of time it takes for  
 80 information to reach higher level recognition stages. The results of this study therefore suggest a complex interplay  
 81 between early and late stages of processing that ultimately manifests in more abstract categorical representations.

82 While it is important to disentangle perceptual features from conceptual representations, the two are inherently  
 83 intermingled. Categorical organisations, such as animacy, are strongly represented partly because they share  
 84 perceptual characteristics, which makes them easier to discriminate. Indeed, inanimate stimuli that share perceptual  
 85 features with animate items evoke brain responses that are similar to other animate stimuli (Bracci, Kalfas, et al.,  
 86 2017). On the other hand, neural responses to animate stimuli that share characteristics with inanimate objects  
 87 (e.g., a starfish) are more confusable with inanimate stimuli (Grootswagers, Ritchie, et al., 2017). Moreover, when  
 88 stimuli are closely matched in shape, the activation patterns can become indistinguishable (Proklova et al., 2016,  
 89 2019). Together, these examples could be taken to suggest that the dichotomy of animacy should be revised to  
 90 more closely reflect, for example, a continuous account of perceptual and conceptual animal typicality (Connolly  
 91 et al., 2012; Grootswagers, Ritchie, et al., 2017; Iordan, Greene, Beck, & Fei-Fei, 2016; Sha et al., 2015).

92 In conclusion, we found that animacy was decodable from texform versions of objects, but that animacy of intact  
 93 objects was more strongly decodable, and at faster presentation frequencies. Information contained in the texform  
 94 versions of the objects thus not fully account for the distinct patterns of neural responses evoked by conceptual  
 95 object categories. These findings suggest that complex interactions between lower and higher levels of visual  
 96 processing mediate the representations of category, which has important implications for disentangling perceptual  
 97 and conceptual representations in the human brain.

## 98 Methods

99 Stimuli, data, and analysis code are available online through <https://osf.io/sz9ve>.

## 100 Participants

101 Participants were 20 volunteers (11 females, 9 males; mean age 24.6, age range: 17-59) recruited from the University  
102 of Sydney in return for payment or course credit. All participants reported normal or corrected-to-normal vision.  
103 Two participants were left-handed. The study was approved by the University of Sydney ethics committee and  
104 informed consent in writing was obtained from all participants.

## 105 Stimuli and design

106 Stimuli were obtained from <https://osf.io/69pbd> (Long et al., 2018). For a full description of the stimulus  
107 generation procedures, see Long et al., 2018. The stimuli were 120 visual objects that were grouped in four  
108 categories: big animals, small animals, big objects, and small objects. This allowed for orthogonal animacy and size  
109 categorisation of the stimuli. All stimuli were matched for average luminance. The stimuli underwent a scrambling  
110 procedure (Long et al., 2018) to generate texform versions of the same objects. All 240 stimuli, 120 intact objects,  
111 and 120 texform versions were used in this experiment (Figure 1).

112 Following the procedure of Long et al., we presented participants with texform versions of the stimuli in the first  
113 half of the experiment, and with intact objects in the second half of the experiment. Participants were all naïve to  
114 the experiment aims and were not informed about the relationship between the texforms and intact images. We  
115 used a rapid serial visual processing paradigm to present the stimuli in fast succession (Grootswagers et al., 2019).  
116 Stimuli were presented in random order in streams at four presentation frequencies: 60Hz, 30Hz, 20Hz, and 5Hz,  
117 always using a 100% duty cycle, following previous work that investigated category decoding at fast presentation  
118 rates (Grootswagers et al., 2019; Mohsenzadeh, Qin, Cichy, & Pantazis, 2018). All stimuli within a category  
119 (texforms/objects) were presented in each stream (i.e., every stream contained 120 images). Stimuli were presented  
120 at 6.8 x 6.8 degrees of visual angle on a grey background and were overlaid with a white fixation dot of 0.2 degrees  
121 diameter (Figure X). During the experiment, participants responded with a button press when the dot changed

colour, which happened between 1 and 4 times during each stream, at random positions in the stream. Each object was presented 30 times in each condition (intact and texform), and at each presentation frequency. The experiment lasted about 40 minutes.

## EEG recordings and preprocessing

Continuous EEG data were recorded from 64 electrodes arranged according to the international standard 10–10 electrode placement system (Oostenveld & Praamstra, 2001) using a BrainVision ActiChamp system, digitized at a 1000-Hz sample rate and referenced online to Cz. Preprocessing was performed offline using EEGLab (Delorme & Makeig, 2004). Data were filtered using a Hamming windowed FIR filter with 0.1Hz highpass and 100Hz lowpass filters and were downsampled to 250Hz. No further preprocessing steps were applied. All analyses were performed on the channel voltages at each time point. Epochs were created for each stimulus presentation ranging from [-100 to 1000 ms] relative to stimulus onset.

## Decoding analysis

We applied an MVPA decoding pipeline (Grootswagers, Wardle, & Carlson, 2017) applied to the EEG channel voltages. The decoding analyses were implemented in CoSMoMVPA (Oosterhof, Connolly, & Haxby, 2016). Regularised linear discriminant analysis (LDA) classifiers were used in combination with a sequence cross-validation approach to decode pairwise image identities firstly between all pairs of texform images, and secondly between all pairs of intact object images. For animacy decoding, an exemplar-by-sequence cross-validation approach was used (Carlson et al., 2013; Grootswagers et al., 2019). That is, a pair of animate and inanimate images from one sequence was used as test data, and classifiers were trained on the remaining images from the remaining sequences. This was repeated for all animate-inanimate pairs and all sequences, averaging the resulting cross-validated prediction accuracies. Real-world size decoding used the same pipeline, with an exemplar-by-sequence cross-validation procedure. All analyses were repeated for each time point in the epochs, resulting in a decoding accuracy over time for every presentation frequency, within subject. The subject-averaged results for each frequency were analysed at the group level.

## Statistical inference

For each decoding analysis, we used Bayesian statistics to determine the evidence for above chance decoding (Dienes, 2011, 2016; Jeffreys, 1961; Rouder, Speckman, Sun, Morey, & Iverson, 2009; Wagenmakers, 2007). For the alternative hypothesis of above-chance (50%) decoding, a JZS prior (Rouder et al., 2009) was set with a scale factor of 0.707 (Jeffreys, 1961; Rouder et al., 2009; Wetzels & Wagenmakers, 2012; Zellner & Siow, 1980). We then calculated the Bayes factor (BF) which is the probability of the data under the alternative hypothesis relative to the null hypothesis. We thresholded  $BF > 3$  as substantial evidence for the alternative hypothesis, and  $BF < 1/3$  as substantial evidence in favour of the null hypothesis (Jeffreys, 1961; Wetzels et al., 2011).

## Acknowledgements

This research was supported by an Australian Research Council Future Fellowship (FT120100816) and an Australian Research Council Discovery project (DP160101300) awarded to T.A.C. The authors acknowledge the University of Sydney HPC service for providing High Performance Computing resources. The authors declare no competing financial interests.

## References

- Andrews, T. J., Watson, D. M., Rice, G. E., & Hartley, T. (2015). Low-level properties of natural images predict topographic patterns of neural response in the ventral visual pathway. *Journal of Vision*, 15(7), 3–3. <https://doi.org/10.1167/15.7.3>
- Bracci, S., Kalfas, I., & Op de Beeck, H. P. (2017). The ventral visual pathway represents animal appearance over animacy, unlike human behavior and deep neural networks. *BioRxiv*, 228932. <https://doi.org/10.1101/228932>
- Bracci, S., & Op de Beeck, H. P. (2016). Dissociations and Associations between Shape and Category Representations in the Two Visual Pathways. *Journal of Neuroscience*, 36(2), 432–444. <https://doi.org/10.1523/JNEUROSCI.2314-15.2016>

- !69 Bracci, S., Ritchie, J. B., & de Beeck, H. O. (2017). On the partnership between neural representations of object  
!70 categories and visual features in the ventral visual pathway. *Neuropsychologia*, 105, 153–164.  
!71 <https://doi.org/10.1016/j.neuropsychologia.2017.06.010>
- !72 Caramazza, A., & Mahon, B. Z. (2003). The organization of conceptual knowledge: the evidence from category-  
!73 specific semantic deficits. *Trends in Cognitive Sciences*, 7(8), 354–361. [https://doi.org/10.1016/S1364-](https://doi.org/10.1016/S1364-6613(03)00159-1)  
!74 6613(03)00159-1
- !75 Caramazza, A., & Shelton, J. R. (1998). Domain-Specific Knowledge Systems in the Brain: The Animate-Inanimate  
!76 Distinction. *Journal of Cognitive Neuroscience*, 10(1), 1–34. <https://doi.org/10.1162/089892998563752>
- !77 Carlson, T. A., Tovar, D. A., Alink, A., & Kriegeskorte, N. (2013). Representational dynamics of object vision:  
!78 The first 1000 ms. *Journal of Vision*, 13(10), 1. <https://doi.org/10.1167/13.10.1>
- !79 Cichy, R. M., Pantazis, D., & Oliva, A. (2014). Resolving human object recognition in space and time. *Nature*  
!80 *Neuroscience*, 17(3), 455–462. <https://doi.org/10.1038/nn.3635>
- !81 Coggan, D. D., Liu, W., Baker, D. H., & Andrews, T. J. (2016). Category-selective patterns of neural response in  
!82 the ventral visual pathway in the absence of categorical information. *NeuroImage*, 135, 107–114.  
!83 <https://doi.org/10.1016/j.neuroimage.2016.04.060>
- !84 Connolly, A. C., Guntupalli, J. S., Gors, J., Hanke, M., Halchenko, Y. O., Wu, Y.-C., ... Haxby, J. V. (2012). The  
!85 Representation of Biological Classes in the Human Brain. *The Journal of Neuroscience*, 32(8), 2608–2618.  
!86 <https://doi.org/10.1523/JNEUROSCI.5547-11.2012>
- !87 Contini, E. W., Wardle, S. G., & Carlson, T. A. (2017). Decoding the time-course of object recognition in the  
!88 human brain: From visual features to categorical decisions. *Neuropsychologia*, 105, 165–176.  
!89 <https://doi.org/10.1016/j.neuropsychologia.2017.02.013>
- !90 Delorme, A., & Makeig, S. (2004). EEGLAB: an open source toolbox for analysis of single-trial EEG dynamics  
!91 including independent component analysis. *Journal of Neuroscience Methods*, 134(1), 9–21.  
!92 <https://doi.org/10.1016/j.jneumeth.2003.10.009>

- 93 DiCarlo, J. J., & Cox, D. D. (2007). Untangling invariant object recognition. *Trends in Cognitive Sciences*, 11(8), 333–  
94 341. <https://doi.org/10.1016/j.tics.2007.06.010>
- 95 Dienes, Z. (2011). Bayesian Versus Orthodox Statistics: Which Side Are You On? *Perspectives on Psychological Science*,  
96 6(3), 274–290. <https://doi.org/10.1177/1745691611406920>
- 97 Dienes, Z. (2016). How Bayes factors change scientific practice. *Journal of Mathematical Psychology*, 72, 78–89.  
98 <https://doi.org/10.1016/j.jmp.2015.10.003>
- 99 Downing, P. E., Jiang, Y., Shuman, M., & Kanwisher, N. (2001). A Cortical Area Selective for Visual Processing  
100 of the Human Body. *Science*, 293(5539), 2470–2473. <https://doi.org/10.1126/science.1063414>
- 101 Grootswagers, T., Cichy, R. M., & Carlson, T. A. (2018). Finding decodable information that can be read out in  
102 behaviour. *NeuroImage*, 179, 252–262. <https://doi.org/10.1016/j.neuroimage.2018.06.022>
- 103 Grootswagers, T., Ritchie, J. B., Wardle, S. G., Heathcote, A., & Carlson, T. A. (2017). Asymmetric Compression  
104 of Representational Space for Object Animacy Categorization under Degraded Viewing Conditions. *Journal*  
105 *of Cognitive Neuroscience*, 29(12), 1995–2010. [https://doi.org/10.1162/jocn\\_a\\_01177](https://doi.org/10.1162/jocn_a_01177)
- 106 Grootswagers, T., Robinson, A. K., & Carlson, T. A. (2019). The representational dynamics of visual objects in  
107 rapid serial visual processing streams. *NeuroImage*, 188, 668–679.  
108 <https://doi.org/10.1016/j.neuroimage.2018.12.046>
- 109 Grootswagers, T., Wardle, S. G., & Carlson, T. A. (2017). Decoding Dynamic Brain Patterns from Evoked  
110 Responses: A Tutorial on Multivariate Pattern Analysis Applied to Time Series Neuroimaging Data. *Journal*  
111 *of Cognitive Neuroscience*, 29(4), 677–697. [https://doi.org/10.1162/jocn\\_a\\_01068](https://doi.org/10.1162/jocn_a_01068)
- 112 Iordan, M. C., Greene, M. R., Beck, D. M., & Fei-Fei, L. (2016). Typicality sharpens category representations in  
113 object-selective cortex. *NeuroImage*, 134, 170–179. <https://doi.org/10.1016/j.neuroimage.2016.04.012>
- 114 Jeffreys, H. (1961). *Theory of probability*. Oxford University Press.



- 15 Kaiser, D., Azzalini, D. C., & Peelen, M. V. (2016). Shape-independent object category responses revealed by  
16 MEG and fMRI decoding. *Journal of Neurophysiology*, 115(4), 2246–2250.  
17 <https://doi.org/10.1152/jn.01074.2015>
- 18 Kaneshiro, B., Guimaraes, M. P., Kim, H.-S., Norcia, A. M., & Suppes, P. (2015). A Representational Similarity  
19 Analysis of the Dynamics of Object Processing Using Single-Trial EEG Classification. *PLOS ONE*, 10(8),  
20 e0135697. <https://doi.org/10.1371/journal.pone.0135697>
- 21 Kiani, R., Esteky, H., Mirpour, K., & Tanaka, K. (2007). Object Category Structure in Response Patterns of  
22 Neuronal Population in Monkey Inferior Temporal Cortex. *Journal of Neurophysiology*, 97(6), 4296–4309.  
23 <https://doi.org/10.1152/jn.00024.2007>
- 24 Konkle, T., & Caramazza, A. (2013). Tripartite Organization of the Ventral Stream by Animacy and Object Size.  
25 *Journal of Neuroscience*, 33(25), 10235–10242. <https://doi.org/10.1523/JNEUROSCI.0983-13.2013>
- 26 Kriegeskorte, N., Mur, M., Ruff, D. A., Kiani, R., Bodurka, J., Esteky, H., ... Bandettini, P. A. (2008). Matching  
27 Categorical Object Representations in Inferior Temporal Cortex of Man and Monkey. *Neuron*, 60(6), 1126–  
28 1141. <https://doi.org/10.1016/j.neuron.2008.10.043>
- 29 Levin, D. T., Takarae, Y., Miner, A. G., & Keil, F. (2001). Efficient visual search by category: Specifying the  
30 features that mark the difference between artifacts and animals in preattentive vision. *Perception &*  
31 *Psychophysics*, 63(4), 676–697.
- 32 Long, B., Störmer, V. S., & Alvarez, G. A. (2017). Mid-level perceptual features contain early cues to animacy.  
33 *Journal of Vision*, 17(6), 20–20. <https://doi.org/10.1167/17.6.20>
- 34 Long, B., Yu, C.-P., & Konkle, T. (2018). Mid-level visual features underlie the high-level categorical organization  
35 of the ventral stream. *Proceedings of the National Academy of Sciences*, 201719616.  
36 <https://doi.org/10.1073/pnas.1719616115>
- 37 Mahon, B. Z., & Caramazza, A. (2011). What drives the organization of object knowledge in the brain? *Trends in*  
38 *Cognitive Sciences*, 15(3), 97–103. <https://doi.org/10.1016/j.tics.2011.01.004>

- McKeeff, T. J., Remus, D. A., & Tong, F. (2007). Temporal Limitations in Object Processing Across the Human Ventral Visual Pathway. *Journal of Neurophysiology*, 98(1), 382–393. <https://doi.org/10.1152/jn.00568.2006>
- Mohsenzadeh, Y., Qin, S., Cichy, R. M., & Pantazis, D. (2018). Ultra-Rapid serial visual presentation reveals dynamics of feedforward and feedback processes in the ventral visual pathway. *ELife*, 7, e36329. <https://doi.org/10.7554/eLife.36329>
- Oostenveld, R., & Praamstra, P. (2001). The five percent electrode system for high-resolution EEG and ERP measurements. *Clinical Neurophysiology*, 112(4), 713–719. [https://doi.org/10.1016/S1388-2457\(00\)00527-7](https://doi.org/10.1016/S1388-2457(00)00527-7)
- Oosterhof, N. N., Connolly, A. C., & Haxby, J. V. (2016). CoSMoMVPA: Multi-Modal Multivariate Pattern Analysis of Neuroimaging Data in Matlab/GNU Octave. *Frontiers in Neuroinformatics*, 10. <https://doi.org/10.3389/fninf.2016.00027>
- op de Beeck, H. P., Haushofer, J., & Kanwisher, N. G. (2008). Interpreting fMRI data: maps, modules and dimensions. *Nature Reviews Neuroscience*, 9(2), 123–135. <https://doi.org/10.1038/nrn2314>
- Proklova, D., Kaiser, D., & Peelen, M. V. (2016). Disentangling Representations of Object Shape and Object Category in Human Visual Cortex: The Animate–Inanimate Distinction. *Journal of Cognitive Neuroscience*, 1–13. [https://doi.org/10.1162/jocn\\_a\\_00924](https://doi.org/10.1162/jocn_a_00924)
- Proklova, D., Kaiser, D., & Peelen, M. V. (2019). MEG sensor patterns reflect perceptual but not categorical similarity of animate and inanimate objects. *NeuroImage*. <https://doi.org/10.1016/j.neuroimage.2019.03.028>
- Rice, G. E., Watson, D. M., Hartley, T., & Andrews, T. J. (2014). Low-Level Image Properties of Visual Objects Predict Patterns of Neural Response across Category-Selective Regions of the Ventral Visual Pathway. *The Journal of Neuroscience*, 34(26), 8837–8844. <https://doi.org/10.1523/JNEUROSCI.5265-13.2014>
- Ritchie, J. B., Bracci, S., & op de Beeck, H. P. (in press). Avoiding illusory effects in representational similarity analysis: what (not) to do with the diagonal. *NeuroImage*. <https://doi.org/10.1016/j.neuroimage.2016.12.079>

- 63 Ritchie, J. B., Tovar, D. A., & Carlson, T. A. (2015). Emerging Object Representations in the Visual System Predict  
64 Reaction Times for Categorization. *PLoS Comput Biol*, 11(6), e1004316.  
65 <https://doi.org/10.1371/journal.pcbi.1004316>
- 66 Robinson, A. K., Grootswagers, T., & Carlson, T. A. (2019). The influence of image masking on object  
67 representations during rapid serial visual presentation. *BioRxiv*, 515619. <https://doi.org/10.1101/515619>
- 68 Rouder, J. N., Speckman, P. L., Sun, D., Morey, R. D., & Iverson, G. (2009). Bayesian t tests for accepting and  
69 rejecting the null hypothesis. *Psychonomic Bulletin & Review*, 16(2), 225–237.
- 70 Schmidt, F., Hegele, M., & Fleming, R. W. (2017). Perceiving animacy from shape. *Journal of Vision*, 17(11), 10–10.  
71 <https://doi.org/10.1167/17.11.10>
- 72 Sha, L., Haxby, J. V., Abdi, H., Guntupalli, J. S., Oosterhof, N. N., Halchenko, Y. O., & Connolly, A. C. (2015).  
73 The Animacy Continuum in the Human Ventral Vision Pathway. *Journal of Cognitive Neuroscience*, 27(4), 665–  
74 678. [https://doi.org/10.1162/jocn\\_a\\_00733](https://doi.org/10.1162/jocn_a_00733)
- 75 Spelke, E. S., Phillips, A., & Woodward, A. L. (1995). Infants’ knowledge of object motion and human action. In  
76 D. Sperber, D. Premack, & A. J. Premack (Eds.), *Causal cognition: A multidisciplinary debate* (pp. 44–78). New  
77 York, NY, US: Clarendon Press/Oxford University Press.
- 78 Teichmann, L., Grootswagers, T., Carlson, T., & Rich, A. N. (2018). Decoding Digits and Dice with  
79 Magnetoencephalography: Evidence for a Shared Representation of Magnitude. *Journal of Cognitive*  
80 *Neuroscience*, 30(7), 999–1010. [https://doi.org/10.1162/jocn\\_a\\_01257](https://doi.org/10.1162/jocn_a_01257)
- 81 Wagenmakers, E.-J. (2007). A practical solution to the pervasive problems of p values. *Psychonomic Bulletin & Review*,  
82 14(5), 779–804. <https://doi.org/10.3758/BF03194105>
- 83 Wardle, S. G., Kriegeskorte, N., Grootswagers, T., Khaligh-Razavi, S.-M., & Carlson, T. A. (2016). Perceptual  
84 similarity of visual patterns predicts dynamic neural activation patterns measured with MEG. *NeuroImage*,  
85 132, 59–70. <https://doi.org/10.1016/j.neuroimage.2016.02.019>

- Watson, D. M., Young, A. W., & Andrews, T. J. (2016). Spatial properties of objects predict patterns of neural response in the ventral visual pathway. *NeuroImage*, 126, 173–183. <https://doi.org/10.1016/j.neuroimage.2015.11.043>
- Wetzels, R., Matzke, D., Lee, M. D., Rouder, J. N., Iverson, G. J., & Wagenmakers, E.-J. (2011). Statistical Evidence in Experimental Psychology: An Empirical Comparison Using 855 t Tests. *Perspectives on Psychological Science*, 6(3), 291–298. <https://doi.org/10.1177/1745691611406923>
- Wetzels, R., & Wagenmakers, E.-J. (2012). A default Bayesian hypothesis test for correlations and partial correlations. *Psychonomic Bulletin & Review*, 19(6), 1057–1064. <https://doi.org/10.3758/s13423-012-0295-x>
- Zachariou, V., Giacco, A. C. D., Ungerleider, L. G., & Yue, X. (2018). Bottom-up processing of curvilinear visual features is sufficient for animate/inanimate object categorization. *Journal of Vision*, 18(12), 3–3. <https://doi.org/10.1167/18.12.3>
- Zellner, A., & Siow, A. (1980). Posterior odds ratios for selected regression hypotheses. In J. M. Bernardo, M. H. DeGroot, D. V. Lindley, & A. F. . Smith (Eds.), *Bayesian statistics: Proceedings of the First International Meeting* (pp. 585–603). Valencia: University of Valencia Press.